49th AIAA Aerospace Sciences Meeting including the New Horizons Forum and Aerospace Exposition
4 - 7 January 2011, Orlando, Florida
AIAA 2011-1311

Lift Generation and Flow Measurements of a Robotic Insect

Z. Hu[1] B. Cheng[1] and X. Deng[2]
School of Mechanical Engineering, Purdue University, West Lafayette, IN, 47907

A 2.86 gram robotic insect with flapping frequencies up to 65Hz was developed to investigate the aerodynamic performance of high frequency flapping wings. The mean lift force was measured by an lever platform with a precision of 0.2mN. Experimental results showed that the lift increased with the flapping frequency in a quadratic manner and was saturated when frequency was beyond 35Hz. A 35 mN lift as well as the highest efficiency was achieved when the robotic insect flapped at 35 Hz. In order to explain the lift saturation, the flow patterns of MAV were investigated by using a DPIV system. Two major issues were found: first, the Leading Edge Vortex (LEV) loses stability and partly sheds away when the frequency is higher than 35Hz; second, the induced flow generated by left and right wings diverge to left and right sides, respectively, which is probably due to the strong tip vortices that were shed into the downwash.

Nomenclature

a	=	length of arm at balanced weight
$\bar{c}$	=	mean chord length
F_{L}	=	lift of MAV
L	=	length of arm at MAV
m	=	balanced weight
m_0	=	standard weight
n	=	flapping frequency
R	=	wing length
$\hat{r}_2^2(S)$	=	non-dimensional second moment of wing area
θ'	=	balanced angle
ρ	=	air density
Φ	=	flapping amplitude

I. Introduction

THERE is an increasing interest in developing flapping-wing micro aerial vehicles (MAV) inspired by insect flight due to their hovering capability and unprecedented maneuverability. Over the past decade research on the insect aerodynamics has revealed fundamental unsteady aerodynamic mechanism in low Reynolds number that is responsible for lift production in insect flight[1].The challenges on robotic insect development include mechanism design, high frequency requirement, and most importantly lift production. In recent years, a few groups have demonstrated lift generation that exceed the body weight of their insect-inspired robots[2]. However, detailed investigation of flow structure around the insect robot, especially in the far field, is still lacking. In this study, we present the design of a robotic insect prototype and its aerodynamic performance. In particular, we measured its lift generation and carried out stereo DPIV experiments to explore the underlying principles that may help develop such MAV devices with desired aerodynamic performance.

[1] Department of Mechanical Engineering, Purdue University.
[2] Department of Mechanical Engineering, Purdue University. Email: xdeng@purdue.edu.

II. Methods and Experimental Setup

A. Robotic Insect

An insect-size flapping robot was developed in the Bio-robotics Lab of Purdue University, shown in Fig.1. The ultimate goal was to develop an autonomous micro aerial vehicle that can hover. It employs horizontal stroke plane similar to most of Dipteral insects. Here we employ a passive wing rotation mechanism, and the pronation and supination of wings results from the inertia and aerodynamics forces during the wing reversal. Mechanical stoppers were employed at the stroke reversal and the angle of attack (AOA) for upstroke and downstroke is 45^{o} during midstroke. The wing stroke angle amplitude is 130^{o}; a frequency of 65Hz could be achieved at 12V power supply; the height is 28mm; the total weight is 2.86 gram (excluding the power supply); the weight for a single wing is 0.04gram with a wing length of 46mm. The slow motions of wings were videotaped by a high speed camera and the kinematics was derived from the camera images. Because of the passive rotation design, there is a lag (about 6% of cycle) between stroke ending and wing flipping (AOA turning point), as shown in Fig. 2.

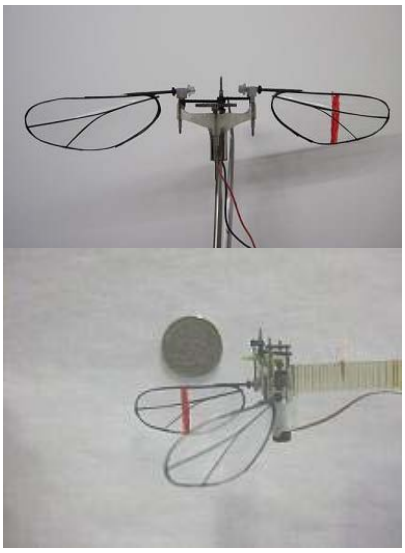

Figure 1. Frontal and side views of robotic insect.

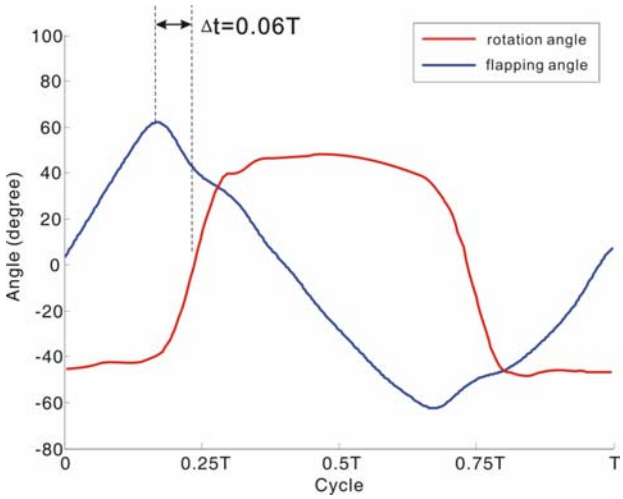

Figure 2. Kinematics measured from wing motion.

B. Force Measurement Platform

Here we designed an Angular Lever Platform to measure the mean lift force (Fig. 3). A lever was setup on to a pivot and can rotate in the vertical plane about the pivot axis. The robot insect was fixed onto the left end of the lever with a distance of L to the pivot; a standard weight m_0 was put on the right part of the lever and its position was adjusted to make the combination (robot, lever and m_0) fully balanced. Here fully balanced means balanced at any angular position for the lever, which also means the mass center of the combination is on the pivot axis. This is critical for the accuracy of the measuring system.

A proper weight m was attached on the left side of lever with a distance of a to the pivot. When the robot flaps at a certain frequency and equation (1) is satisfied, the lever can recover the balance at a particular angular position θ' after several swings:

$$mga > LF_l \tag{1}$$

Considering both the pre-balance and the new balance, the lift force generated at this moment can be calculated by:

$$F_L = \frac{mga\cos\theta'}{L} \tag{2}$$

This lever platform can also be used to measure the side force generated by a single wing. For doing that the MAV with a single wing should be rotated by 90 ^{o} so that the wing is pointing downward.

Although the pivot generates very limited torque, the wire connection between the actuator and the DC power supply may have some undefined force transferred to the lever therefore cause measurement errors. We used two solutions to minimize this effect: 1) use thin copper wire of 0.13mm diameter (gauge 36) with max current of 500mA, since the actuator absorbs current no larger than 400mA; 2) Attach the wire to the lever from the pivot point. Therefore even if we have some considerable tensions along the wire, the torque generation could still be zero.

To check the accuracy of the measuring system, we put a small mass on the position close to the robot under the pre-balance condition, and found that a mass of 0.02 gram is able to break the balance. Thus the sensitivity of the system is up to 0.02 gram. Considering the robot can generate lift forces above 1 gram, the system error is less than 2%.

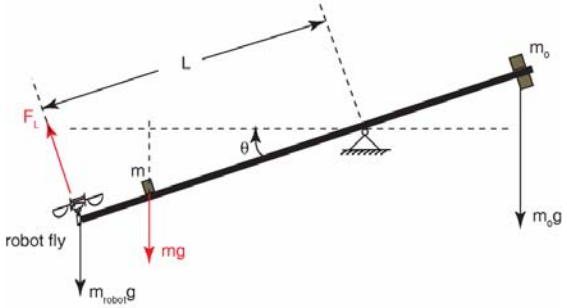

Figure 3. The Angular Lever Platform

C. DPIV System

The stereo DPIV system was manufactured by TSI Inc. The basic setup was shown in Fig. 4A. We used a dual-cavity pulsed YAG laser (120-mJ) at 532 nm wavelength to illuminate a flow field sheet of 1mm thickness. The air was seeded with submicrometre-sized particles of olive oil vapor, generated by a Laskin nozzle. Particle illumination was recorded with a pair of PowerView Plus 2MP, 1.6K x 1.2K pixel resolution, high Quantum Efficiency, low noise Digital CCD cameras equipped with 50mm/F1.8 camera lens. Laser Pulse Computer controls the Synchronizer with time resolution of 1ns and triggering channels for input and output, External Trigger TTL input and RS-232 communication. Data are processed by Insight 3G Image Capture, Analysis, and Display Software Platform built on Net technology with parallel processing capability and integrated TecPlot data presentation. A phase lock circuit was developed with a laser pointer and an optical sensor. The circuit will send a TTL pulse to the Synchronizer each time the wing passes the beam of laser pointer.

The side view PIV test will be carried out at 3 wing spanwise positions as shown in Fig. 4B. The laser sheet will intersect the wing at positions of 55%, 65% and 75% wing length from wingbase and are considered as the most significant lift generation area along the wing.

III. Results and Discussion

D. Force Measurement and Calculation

We measured the lift forces with the supply voltage ranging from 3.5V to 8.5 V. in the mean time flapping frequency was also recorded by using a tachometer. The results are summarized in Fig. 5A. We can see that the flapping frequency increases almost linearly with the voltage supply, which is consistent with the DC motor characteristics. The highest frequency of 42 Hz was recorded with 9V voltage supply. We could run the robot at

higher voltage (12V) and higher frequency (up to 65Hz), but that would bring the irregular wing deformation and the efficiency would drop considerably.

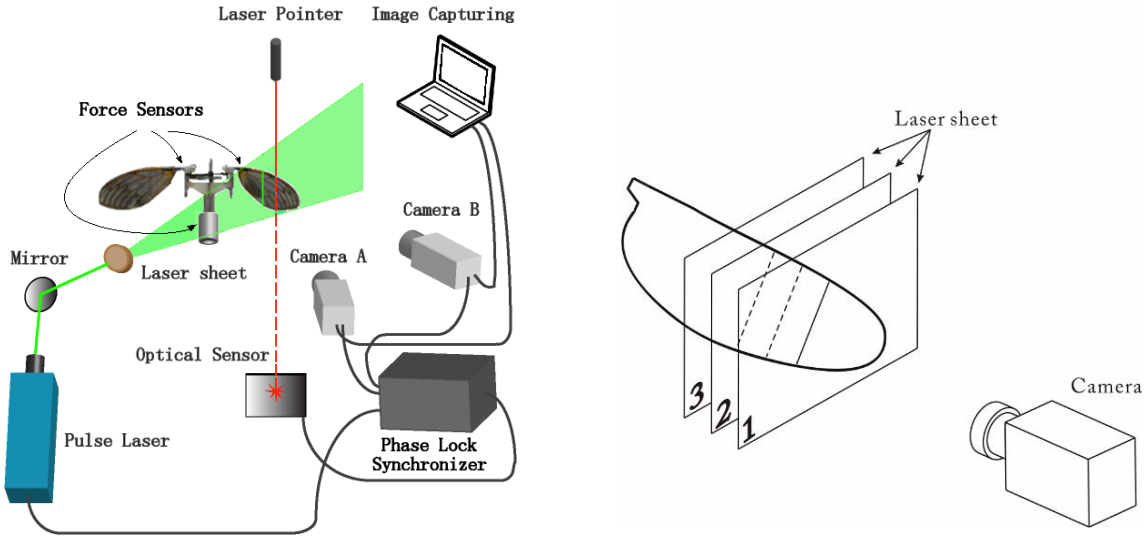

A B

Figure 4. A) The DPIV system setup; B) The sections for side view PIV test.

The mean lift generated by the robotic insect under different flapping frequency is shown in Fig. 5B. The results show that in general, the lift increases with the frequency in a quadratic manner. However, as the frequency goes higher than 35Hz, the lift force goes into a state of saturation, while the side force increases dramatically. In later PIV section, we further investigated the flow patterns when frequency was 30, 36 and 42Hz respectively. Results showed that the saturation might be due to LEV shedding and wake divergence which happens in the higher frequency, as shown in Fig. 6 and Fig 7. The 35Hz might be an upper limit for the wings to keep the LEV stable; therefore we consider this number as a threshold for the MAV with the current settings.

The robot insect shows a good performance of lift force as well as the efficiency when 7.5 V was supplied. The lift force at this moment is 35.2 mN, which is large enough to support the weight of the body (excluding the power supply).

The lift coefficient was calculated according to the following equation:

$$C_{\mathrm{L}} = \frac{F_{\mathrm{L}}}{\rho R^3 \bar{c} \hat{r}_2^2(S) \left| \overline{\frac{d\phi}{dt}} \right|^2} \tag{3}$$

where ρ is the air density, R is wing length (48mm), $\bar{c}$ is mean chord length (13mm), $\hat{r}_2^2(S)$ (0.36) is the non-dimensional second moment of wing area, F_{L} is measured lift (for a wing pair), $\left| \overline{d\phi/dt} \right|$ is the mean wing angular velocity, which is approximated by $2\Phi n$, where Φ is flapping amplitude and n is flapping frequency. Fig. 5C shows the lift coefficient at different flapping frequency, the mean lift coefficient is at 1.91. For the tested frequency which ranges from 18 to 40Hz, the Reynolds number (3400 to 7500) is also close to the one of hawkmoth (Manduca Sexta) flight. Assuming the body weight at 1.5 gram, a hawkmoth need to achieve a mean lift coefficient at about 2.5 in order to hover, which is higher than the one measured in the current experiment. This might reflect some wing morphological and kinematical difference between the hawkmoth and the robotic insect. Specifically, hawkmoth flap asymmetrically for up and down strokes with a tilted stroke plane, and the robotic insect robot flaps horizontally. And hawkmoth wings generally have wing twist and flexibility which could enhance the lift production at high angle of attack. Therefore, this result suggests that more careful design of wing flexibility and shape as well as kinematics could very likely increase the lift production.

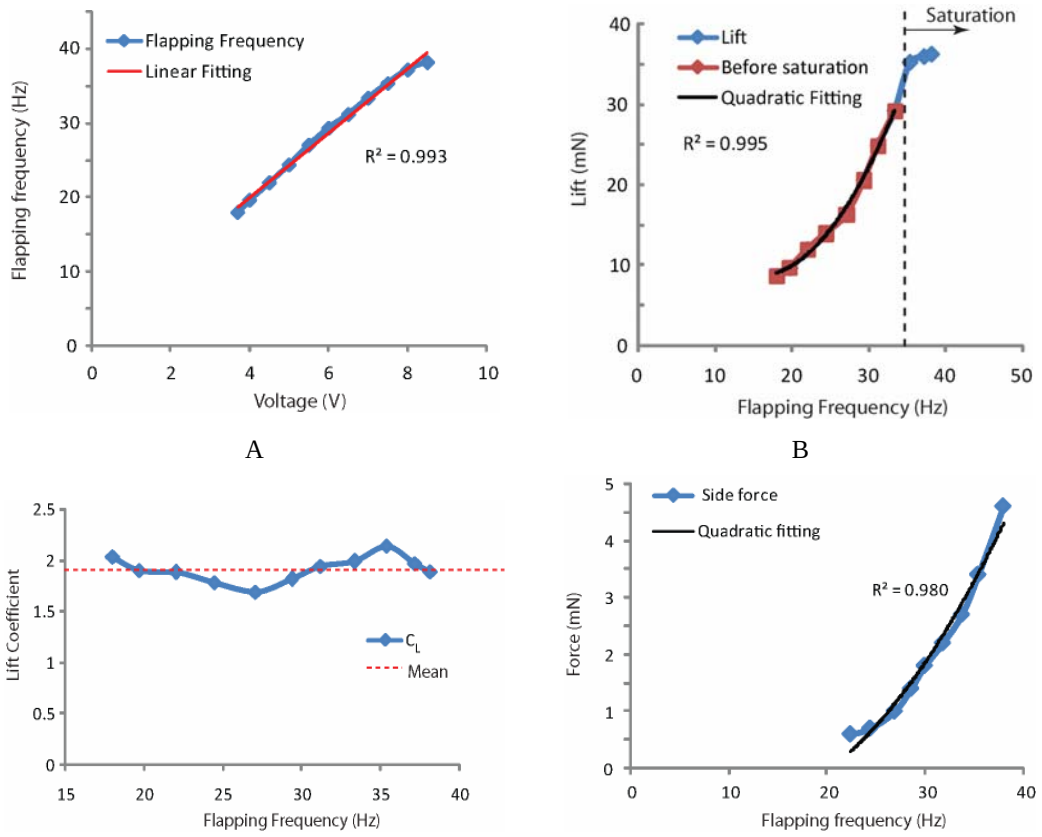

Figure 5. A) The flapping frequencies used in experiments; B)The lift force measured at different flapping frequencies; C)The Mean lift coefficients at different flapping frequencies; D)The side forces measured at different flapping frequencies.

E. Flow Visualization Analysis

In order to explore the reasons for the lift saturation as the frequency goes above 35Hz, we carried out PIV experiments to visualize the vortex and induced flow patterns at different frequencies (30, 36 and 42Hz). The LEV was examined from the side view PIV at 3 spanwise positions. They have a distance of 55%, 65% and 75% wing length from wingbase and are considered as the most significant lift generation area along the wing. The wake right below the wings was also studied in the frontal view PIV with a view section passing the middle of wing stroke. The results revealed two major findings: first, the LEV became more unstable and detached from leading edge at high frequencies; second, the downwash under the flapping wings diverged sideward in the frontal view at high frequencies.

Figure 6 presents the LEV pattern at 3 spanwise sections and 3 frequencies. The LEV firmly attaches to the leading edge of the wing with little shedding at 30Hz. When wings flap at 36Hz and 42Hz, another vortex in negative sign can be clearly found at a lower position. We believe it is a detached portion of LEV which lost its stability during the early stroke. The circulations of the attached and detached LEV were calculated and compared. About 20~23% of LEV was shed at 36Hz and the detachment ratio increased to 29~35% at 42Hz.

Experimental and computational studies in previous years have identified the LEV as an important feature of the flows created in flapping flight. The lift force can be enhanced as LEV keeps attaching to the wing. Polhamus[3] described a simple way to account for the enhancement of lift by LEV: flow separates at the sharp leading edge of wing, leading to the formation of a leading edge vortex. In this case, an analogous suction force normal to the plane of the wing develops, thus adding to the potential force and consequently enhancing the lift component throughout the stroke cycle.

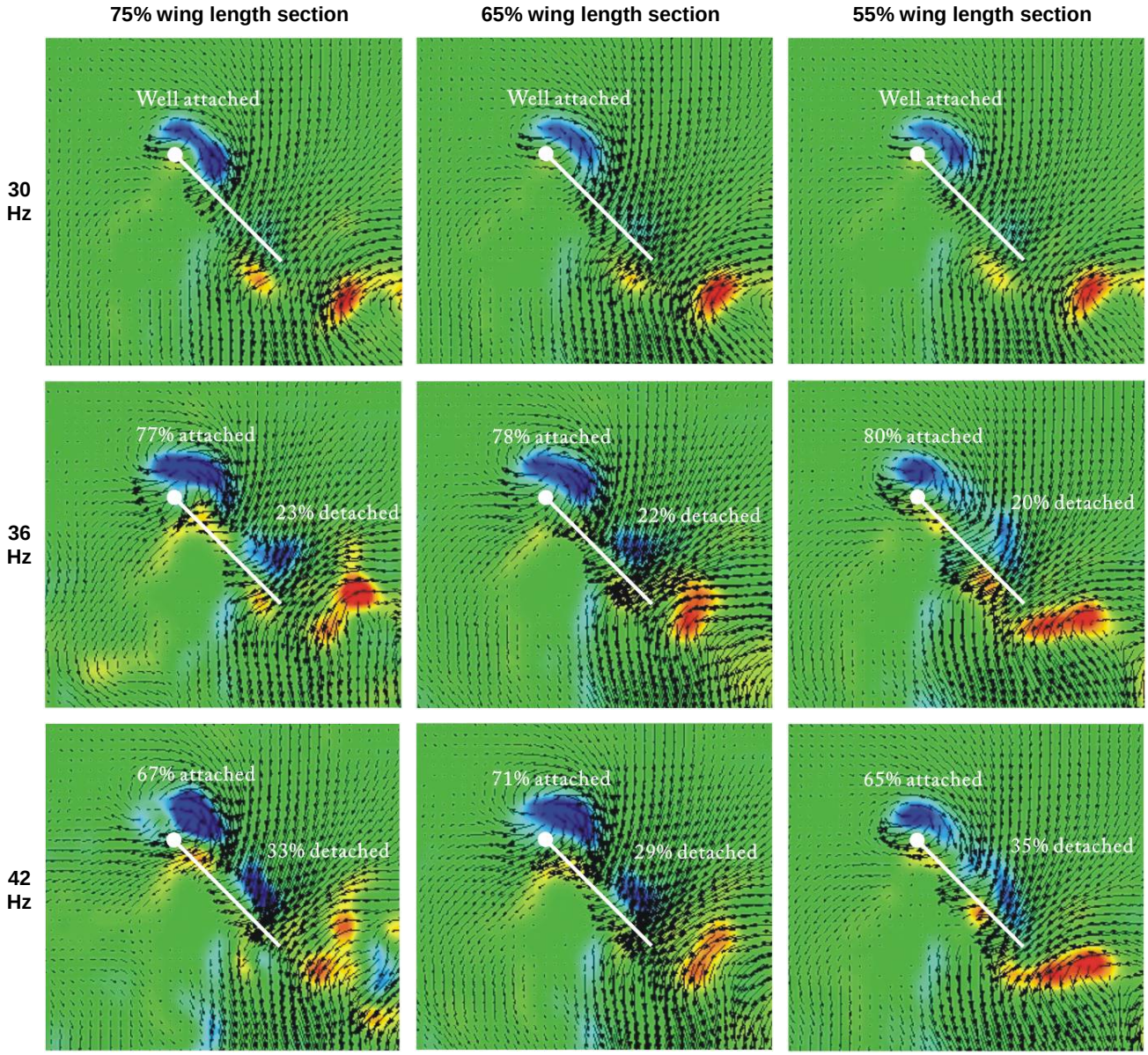

Figure 6. The LEV patterns from side view during the mid stroke. Each PIV result is an average of 10 instantaneous results measured under the same condition. The percentages of attached LEV and detached LEV were derived according to their magnitudes of circulation.

Although many insects or birds fly with a stable LEV[4-6], it is interesting to find that the LEV on our MAV loses the stability when the frequency goes higher than 35Hz (Fig. 6). This is reasonable in the way that as the flapping speed increases, the LEV keeps expanding on the wing until its vortex energy balance is broken. According to the LEV suction analogy, the lift production on the wing will suffer a loss due to the LEV shedding. Hence the lift measurements slow down its growing at 35 Hz, although the flapping speed was comparatively high. Apparently this is a detrimental situation that should be avoided in MAV design. A new LEV grows from the leading edge after the old one's shedding, which could recover a part of lift force.

The above speculation can be supported by a study from Dickinson and Gotz[7]. They showed the time trace of lift production on a wing model that started a translational moving from rest. During the time of maximal lift production (2–2.5 chord lengths), the vortex remains on the upper surface of the wing. After about 4 chord lengths of travel, the vortex becomes extended rearward and is eventually shed from the profile. As this leading edge vortex is being shed, a vortex of opposite sign develops on the trailing edge. This alternating pattern continues, resulting in a von Karman street, whose time history is tightly correlated with the oscillations of the force records.

A stable LEV probably indicates that the stalling of the wing is being delayed. During the wing strokes, the coming freestream is cut by the sharp leading edge and separates from the wing surface. It will reattach to the wing surface due to the existence of a stable LEV and smoothly flow along the trailing edge. Therefore the Kutta condition can be satisfied and all the circulation around wing will generate a circulatory lift according to Kutta-Zhukhovsky theorem. If the LEV becomes unstable and starts shedding, like the case of 36 and 42Hz flapping in Fig. 6, the flow reattachment is no longer available and the Kutta condition breaks down. As a result, the lift will drop and the drag will increase, because the downwash can not be produced consistently. At this moment, the stall happens.

In a case of airfoil in 2D linear motion, the stall occurs when its AOA exceeds a threshold value which is called critical AOA in fluid dynamics. The threshold is typically 15^{o} and may vary around depending on Reynolds numbers and geometry factors. While the AOA employed by the MAV in the study is well above 15^{o} and it can still avoid stalling at low flapping frequencies (30Hz). The 3D wing motion may be responsible for the stall delay. Vandenberg and Ellington[8] discovered the existence of spanwise flow in hawkmoth flight and the spanwise flow could stabilize the LEV attachment.

On the other hand, the spanwise flow can transfer part of LEV circulation and feed it into a tip vortex which will be shed from wing tip, as it is shown in Fig.7 that a blue tip vortex on the left and a red tip vortex on the right are shed one wing chord length below the wing tip. The strength of the tip vortex increases dramatically as the frequency goes up to 36Hz and 42Hz. Migratory birds usually fly in a V formation to take advantage of tip vortices of front bird. The upwash of the tip vortex makes the bird easier to

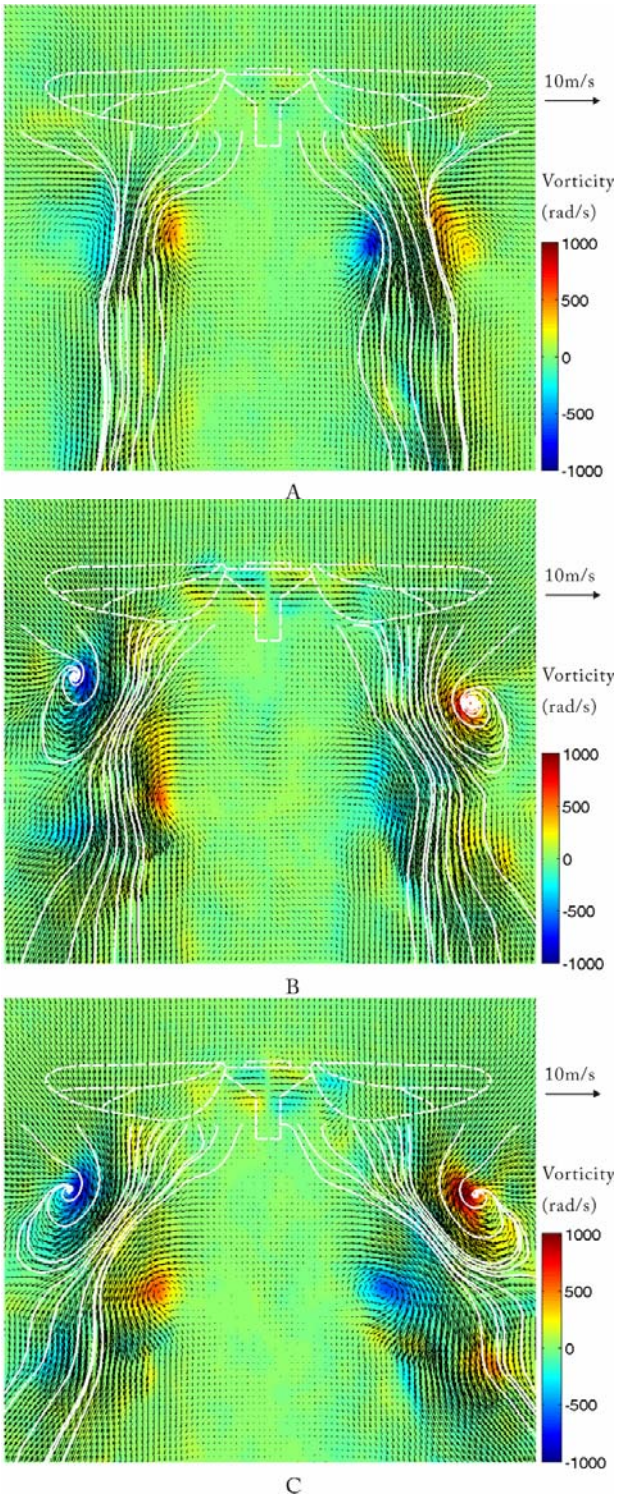

Figure 7. The downwash streamline pattern at the end of stroke in frontal view PIV. A, B, and C correspond to the results of 30, 36 and 42Hz. Each result is an average of 10 instantaneous results measured under the same condition.

support its own weight so as to improve efficiency on migration flights.

Unfortunately for the MAV in this study, the tip vortices may have some negative influences on lift production. The vortices spin at very high speed and contain considerable energy which will finally be shed into the wake and is not possible to be recycled. Besides, the cores of tip vortices are regions of low pressure. It is detrimental for lift generation since these low pressure cores are located below the wing for most of time. Most importantly, the strong tip vortex will redirect the induced flow by driving the downwash to sideways.

As we can see from Fig. 7, both the left and right streamlines of downwash show a vertical pattern at a low frequency (30Hz). As flapping speed goes higher, the streamlines start to diverge sideways. The left ones were more inclined to left and right ones were flowing to right. Such a kind of divergence of downwash indicates that there is a considerable horizontal momentum put into fluid by the two wings. Theoretically, the lift production on the wings is proportionate to the downward momentum put into the fluid, while the horizontal momentum only accounts for side forces. Therefore, as the frequency goes higher, the side force of MAV increases dramatically, while the lift tends to be saturated.

IV. Conclusion

A robotic insect with flapping frequencies up to 65Hz was developed for testing aerodynamics. Lift measurements showed that the lift increased with the flapping frequency in a quadratic manner and was saturated when frequency was beyond 35Hz. A 35 mN lift as well as the highest efficiency was achieved when the robotic insect flapped at 35 Hz. The flow patterns of MAV were investigated by using a DPIV system. Results show that the Leading Edge Vortex loses the stability and partly sheds away from wings when the frequency goes higher than 35Hz. Besides, the induced flow generated by left and right wings diverges to left side and right side respectively. The reason for the LEV shedding is still unclear, but the wake divergence is probably due to the strong tip vortices that were shed into the downwash. In the future, seeking solutions to minimize the wake divergence and stabilize LEV could be significant in order to promote the lift production on the MAV.

Acknowledgments

We thank Giovani Barbera and Jesse Roll for their help with the phase lock design and seeder generator as well as the PIV experiments. This work was supported in part by National Science Foundation Award #0545931.

References

1 **Dickinson, M. H., Lehmann, F. O. & Sane, S. P. Wing rotation and the aerodynamic basis of insect flight. *Science* 284, 1954-1960 (1999).**

2 **Wood, R. J. 1576–1581 (San Diago, CA, *Proc. IEEE/RSJ Int. Conf. Intell. Robots Syst,* Oct, 2007).**

3 **Polhamus, E. Vol. 8 193-199 (*J. Aircraft,* 1971).**

4 **Warrick, D. R., Tobalske, B. W. & Powers, D. R. Aerodynamics of the hovering hummingbird. *Nature* 435, 1094-1097, doi:10.1038/nature03647 (2005).**

5 **Muijres, F. T. *et al.* Leading-edge vortex improves lift in slow-flying bats. *Science* 319, 1250-1253, doi:10.1126/science.1153019 (2008).**

6 **Willmott, A. P., Ellington, C. P. & Thomas, A. L. R. Flow visualization and unsteady aerodynamics in the flight of the hawkmoth, Manduca sexta. *Philosophical Transactions of the Royal Society of London Series B-Biological Sciences* 352, 303-316 (1997).**

7 **Dickinson, M. H. & Gotz, K. G. Unsteady aerodynamic performance of model wings at low reynolds-numbers. *Journal of Experimental Biology* 174, 45-64 (1993).**

8 **VandenBerg, C. & Ellington, C. P. The three-dimensional leading-edge vortex of a 'hovering' model hawkmoth. *Philosophical Transactions of the Royal Society of London Series B-Biological Sciences* 352, 329-340 (1997).**